Chitosan Silver Nanofibers for Wound Healing

Posted on March 11, 2025

Abstract

The use of electrospinning to create dressings for wounds has gained more scientific attention over the past few years. In addition to the method's ease of use, versatility, and scalability, the electrospun nanofiber produced has extraordinary characteristics such as the ability to absorb wound exudate, flexibility, high porosity, and a high surface-to-volume ratio. This study aims to synthesize and characterize chitosan-based electrospun nanofibers that are rich in environmentally benign AgNPs. The environmentally friendly silver nanoparticles were created utilizing a green method involving plant extracts and electrospun from a chitosan solution. Using Fourier-transform infrared spectroscopy (FTIR), X-ray diffraction (XRD), scanning electron microscopy (SEM), and differential scanning calorimetry analysis (DSC), the resultant nanofibers were examined for their morphology, structure, and chemical makeup. The effective integration of Ag nanoparticles into the chitosan nanofibers was established by the XRD and FTIR analyses. Because the polymer solution has a high degree of surface tension, the CT + PEO + AgNP combination of electrospun nanofibers demonstrated excellent-quality fibres with a typical fibre diameter of about 150 nm.

Introduction

Skin injuries are a serious healthcare issue that has high rates of mortality and morbidity. Despite improvements in dressings for injury systems over the course of the last few decades, the limited efficacy of available treatments continues to be an issue (Mirhaj et al., 2022; Pourshahrestani et al., 2020). Since bacteria that are impervious to antibiotics are becoming more prevalent, using medications to avert and treat wound infections is inefficient (Tan et al., 2020). It also comes at an additional expense to the sufferer and society. Investigating cutting-edge methods to develop novel technologies with enhanced efficacy for accelerating skin regeneration and wound healing is, therefore, essential. Numerous experimental studies on a variety of cells, including mesenchymal stem, bone and cartilage, neuron, and heart cells, have shown that electrical stimulation has an impact on the main behaviours of cells, including adherence, differentiation, proliferation, and motility (Vandghanooni and Eskandani 2019; Chen et al., 2019).

In recent years, the scientific community has become increasingly interested in using electrospinning to make wound dressings (Shahid et al. 2021; Stoica et al. 2020). Due to their nanoscale properties, these membranes can imitate the matrix structure, facilitating migration, proliferation, and cell

Copyright © 2026 Academic Master.

adhesion, as well as helping to regenerate injured skin (Anjum et al., 2022). Additionally, the enormous specific surface area and many holes of nanofiber scaffolds render them a great base for cell attachment. Additionally, the tightly connected pore structure and small pore size allow for oxygen and water penetrability while also preventing bacterial infiltration and the spread of diseases. The capacity of these membranes to incorporate bioactive components that directly contribute to the wound's recovery while ensuring their continued delivery to the area of injury is further evidence of their fascinating potential to serve as advanced biologically responsive dressings. These characteristics all have a role in how well a wound heals. Electrospinning is a productive method that yields continuous nanofibers with typical sizes between a few tens and hundreds of nanometers, which are between 100 and 10,000 times smaller than fibres made by melt or solution spinning (Cui et al., 2021).

A natural-based and disposable substance could be used in the creation of ecologically friendly dressings for injuries due to the increased need for environmentally conscious options in the wound care sector. The natural biopolymer chitosan, which is produced via chitin deacetylation, is found on the shells of crustaceans, algae cell walls, fungi, etc. (Elsoud et al., 2022). This natural polysaccharide has drawn a lot of interest in a range of biomedical applications due to its well-known antibacterial activity against a wide range of fungi and bacteria, non-toxicity, non-immunogenicity, high biocompatibility, and biodegradability. N-acetyl glucosamine, a monomer found in chitosan, has been shown to encourage coagulation, trigger the proliferation of cells, and hasten the wound healing process.

Additionally, adding silver nanoparticles (AgNPs) to wound dressings has been shown to have a remarkable potential for speeding up the healing process. AgNPs have special antibacterial qualities that enable them to be effective against a variety of diseases that can obstruct the healing process. AgNPs were created using eco-friendly processes, which is in line with the increased focus on eco- and sustainably produced materials in the field of nanomedicine. The goal of this study is to create and analyse electrospun nanofibers made of chitosan that are loaded with ecologically friendly AgNPs. The resulting nanocomposite dressing is anticipated to provide a variety of benefits, including accelerated wound healing, tissue regeneration, and antibacterial activity. This work, which explores the potential of these innovative wound dressings for quicker and enhanced wound healing results, aims to close the gap between advanced nanotechnology and wound care in this setting. This inquiry seeks to provide insightful information into the design and development of next-generation wound dressings, providing creative solutions to the urgent problems of chronic wound treatment.

Materials and Methods

2.1 Natural silver nanoparticle synthesis

Aloe vera, *Ocimum tenuiflorum* (Holy Basil), *Syzygium cumini* (Jamun), *Ficus carica* (Fig), and *Tridax procumbens* are among the medicinal plants whose leaves were gathered and whose extracts were

made using a methanol solution. A common approach involved combining 5 mL of the leaf extract with 50 mL of a room-temperature aqueous solution containing $1\times10.^{-3}$ M $AgNO_3$. The solution turned grey-black after 60 minutes, indicating that silver nanoparticles (AgNPs) had successfully formed.

2.2 Electrospinning

Separate solutions of polyethene oxide (PEO) and chitosan were made, each with a particular concentration: 8% (w/v) PEO and 3% (w/v) chitosan. These solutions underwent painstaking optimisation. They were then merged 50/50 and blended together using the sonication technique to produce a composite sample known as CT + PEO. A composite sample known as CT + PEO + AgNP was created by adding a 4% solution of silver nanoparticles (AgNP) made using green synthesis in a separate stage to the CT + PEO polymer solution. All samples were processed using a pump, and the needle's tip received a 15 kV power supply. At a flow rate of 1 mL/h, the nanofibers had been dropped onto a collection vessel that was 15 cm beyond the needle. The revolving collector was surrounded by an aluminium sheet coated with nanofibers and connected to a negative electrode by a wire. The spinning process took place at 40%–60% RH and a temperature of 25°C. The flow of the solution was aided by gravity, while the spinning produced electrostatic forces. Any acetic acid that remained after spinning was successfully removed by washing the nanofiber matrix until the neutral pH was reached. The nanofibers were eventually prepared for characterisation examination by being desiccated for 24 hours in a vacuum oven.

2.3 Characterization

2.3.1 SEM analysis

The physical structure of the nanofiber surfaces was examined using scanning electron microscopy (SEM). The Auto Fine Platinum Coater was used to apply a platinum layer to the stub prior to imaging. The morphological structure and fibre diameter were investigated using an SEM with a 10 kV acceleration voltage. Preceding the experiment, the nanofiber samples were given a gold sputter coating in an argon atmosphere to make them electrically conductive. Porosity and fibre diameter were also calculated.

2.3.2 XRD Measurements.

A STADI-P diffractometer, made by Stoe in Darmstadt, Germany, was used to gather data on X-ray powder diffraction for the sample CT + PEO + AgNP. The diffractometer used transmission-geometry-configured Ge(111) crystals to filter monochromatic Cu Kα light with a wavelength of 1.54056Å. The X-ray source used 40 mA and 40 kV to operate. The nanofibers were put between two acetate-cellulose foils in order to get them ready for analysis. A Mythen 1K detector made by Dectris in Baden,

Switzerland, was used to capture the diffraction pattern. Data points were collected at intervals of 0.015° and covered the 2θ range between 3° and 61°. Over the course of 60 seconds, each data point was integrated at each 1.05° increment in the scanning range.

2.3.3 FTIR

The Fourier transform infrared spectrum (ATR FTIR) (Perkin-Elmer, USA) was used to determine the chemical collective of the electrospun nanofibers. Small sections of the sample nanofibers were cut, combined with KBr, and then constrained to form pellets. With a tenacity of 2 cm^{-1}, measurements were made between 400 and 4000 cm^{-1}.

2.3.4 DSC analysis

On the basis of the endothermic process, the thermal examination of nanofibrous materials was carried out using differential scanning calorimetry (DSC) (METTLER TOLEDO, Switzerland). With nitrogen flowing at an intensity of 50 mL per minute, the samples underwent heating from the ambient temperature to 250°C at a frequency of 10°C per minute.

Result and discussion

Maintaining wounds is essential, especially for diabetic patients and people who have suffered burns. The wound becomes a part of the skin after it has been created, and bacteria thrive there. Depending on the wound's location, kind, and management, the healing process can begin. Both external and internal factors have the potential to obstruct the healing process. Following the release of cytokines that cause cell migration and proliferation, the internal prerequisite step in wound healing occurs. Reactive oxygen species and bacterial infections are significant hindrances to the wound-healing process that can delay each phase.

Chitosan's stiff D-glucosamine units of repetition and propensity to establish inter- or intramolecular bonds of hydrogen make it difficult to fabricate into nanofibrous structures. Typical organic solvents. Chemical manipulation is an alternate strategy to improve the dissolution and spinnability of chitosan, as demonstrated by Geng et al. in 2005. However, a more straightforward method for refining the chitosan electrospinning is by amalgamating it with another polymer, whether of synthetic or natural origin, such as PEO, or by incorporating green-synthesized nanoparticles, as suggested by Bösiger et al. in 2018. These advancements have given rise to a novel category of wound dressings composed of chitosan-based nanofibers. These wound dressings exhibit exceptional properties, including superior biocompatibility, biodegradability, porosity, and antimicrobial activity, as highlighted by the work of Antunes et al. in 2015.

3.1 SEM analysis

Significant morphological alterations in nanofibrous mats were seen in SEM pictures. Figure 1 displays the exterior architecture of the developed nanofibers, which demonstrates that every structure has nanoscale fibres similar to the structural network present in native tissue (Khodadoust et al., 2018). Because of the elevated tension on the exterior, the CT + PEO + AgNP combination among the electrospun nanofibers showed high-quality fibres with little bead formation. Ag NPs increased the electrospinnability of the polymer solution, producing non-beaded fibres that were more consistent and uniform. Ag NPs were added to the nanofiber surface, which enhanced the charge density and reduced the fibre diameter. The rise in charges of electricity on the polymer droplet's interface at the site of injection due to increased conductivity was what led to the emergence of a Taylor cone. As a result, improved conductivity increased the polymer solution's ability to stretch and led to the electrospinning process' creation of fibres with smaller diameters (Angammana and Jayaram, 2011; Jirofti et al., 2021).

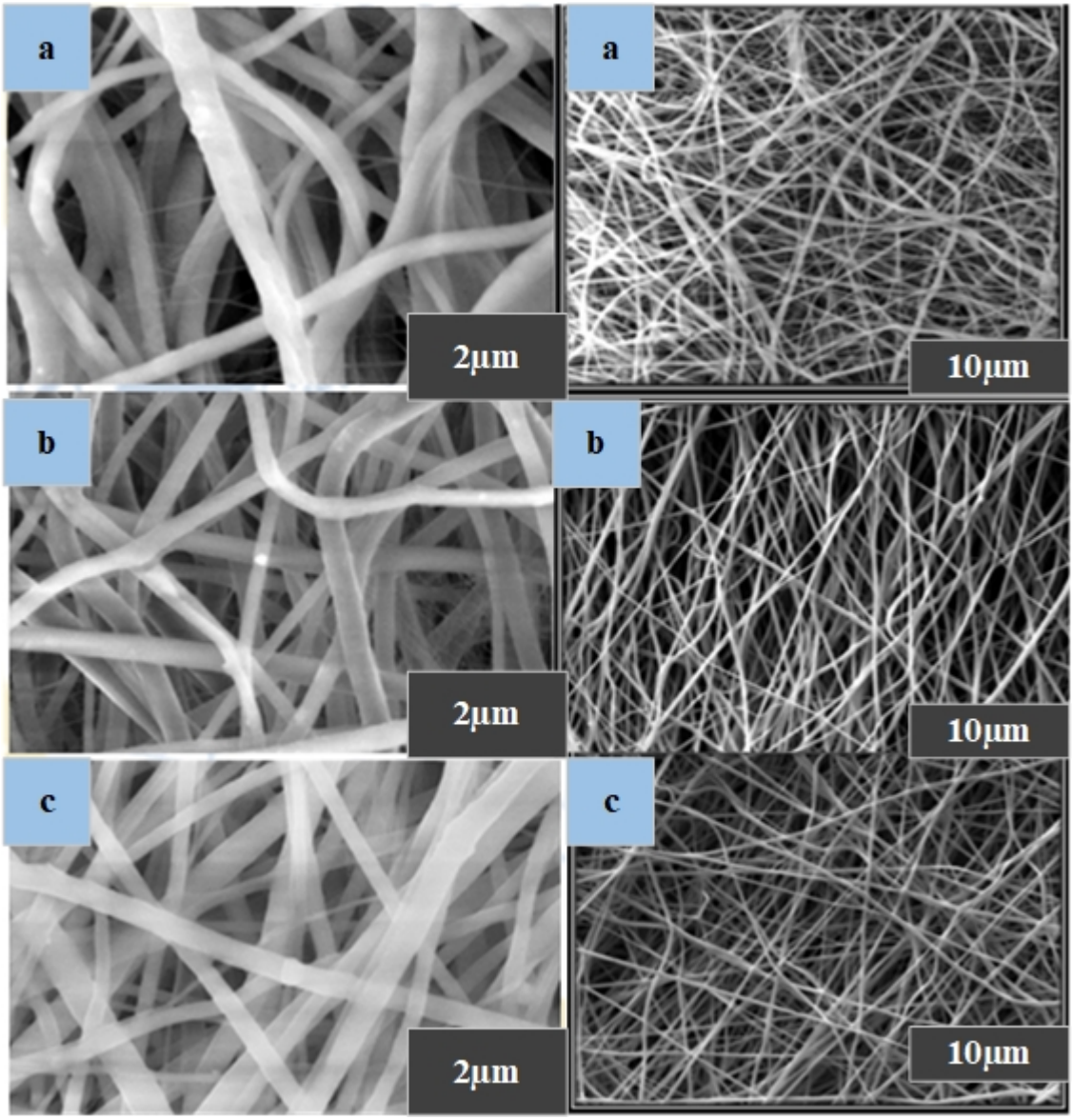

Figure 1: SEM images of the samples. (a) CT; (b) CT + PEO; and (c) CT + PEO + AgNP.

3.2 Fiber density and porosity measurement

Silver nanoparticles were added to the Chitosan PEO polymer solution to help the electrospinning process run smoothly and produce homogeneous, bead-free nanofibers with a size in the nanoscale range. For chitosan (CT) and chitosan with polyethene oxide (CT + PEO), the average fibre sizes were determined at 92 nm and 132 nm, respectively. It is noteworthy that the addition of green-synthesized nanoparticles to the polymer solution caused a significant increase in fibre diameter, which increased to an average of 158 ± 25 nm and surpassed the dimensions of the control nanofibers (figure 2). With an ideal fibre thickness of around 150 nm, this uninterrupted and seamless structure is particularly suited for incorporating silver nanoparticles for potential uses in the therapy of microbial-infected injuries. As reported by Ganesh et al. in 2016 and Shi et al. in 2016, The unique

characteristics of these nanofibers imply that the silver nanoparticles have created crosslinks with the scaffold through hydrogen attachment, inhibiting the absorption of water and the expansion of drug-loaded nanofibers.

Chitosan (CT) and Chitosan with Polyethylene Oxide (CT + PEO) nanofibers were reported to have mean porosities of 85 ± 0.39 and 82 ± 0.46, respectively. The porosity, on the other hand, marginally dropped to 79 ± 0.58 in the case of the AgNP-loaded Chitosan with Polyethylene Oxide (CT + PEO) nanofibers (figure 2). As stated in the work by Srivastava et al. in 2019, the porosity examination of nanofibers loaded with Ag nanoparticles revealed a typical porosity of around 80%, a parameter that is crucial for promoting cell proliferation, adhesion, and growth. The synthesis of homogenous, bead-free nanofibers with enhanced diameter was made possible by the addition of silver nanoparticles to the Chitosan PEO polymer solution, making them suitable for drug encapsulation in wound healing applications. The nanofibers also kept a desirable amount of porosity, which increased their capacity for encouraging cell proliferation and tissue regeneration. This study opens up a viable new path for the biomedical engineering industry to create cutting-edge materials.

3.3 Characterization

Figure 3 illustrates how FTIR analysis has been utilized to investigate the distinct chemical links discovered inside the created nanofiber samples. A peak in the spectrum from 3000 to 3400 cm^{-1} in the sample CT + PEO + AgNPs denotes the presence of amide and hydroxylation bonds connected to the functional groups of silver nanoparticles derived from plants. On the other hand, pure chitosan samples often show modest crests in the 3000–3400 cm^{-1} region, which can be attributed to the polysaccharide molecules' intermolecular hydrogen bonds as well as the extended oscillations of their OH–O and N–H bonds. However, because of incomplete interactions with the solution, these peaks were somewhat muted. We did detect N-H and OH/O absorption bands at 3328 cm^{-1} in our experiments. As previously reported by Ridolfi et al. in 2017, samples of CT and CT + PEO also exhibited similar properties, with absorption bands for carbonyl C=O-NHR and amine -NH_2 at 1668 and 1489 cm^{-1}, respectively.

According to Pakravan et al. (2012), the combined solutions of PEO and chitosan with a 50:50 composition displayed peaks corresponding to C-O-C stretching vibrations in the series of 900 to 1200 cm^{-1}, with the highest intensity detected at 1096 cm^{-1}. This is in line with the results of our experiments, where we also found peaks at 1467 cm^{-1} (related to C-H bonding) and 1338 cm^{-1} (related to methyl group's C-H deformation). The 900 kDa molecular weight of PEO used in this investigation may have contributed to the OH absorption bands' lack of prominence in our experimental setup.

The FTIR analysis findings indicate the successful electrospinning of the chitosan polysaccharide chains, as evidenced by the occurrence of OH absorption bands at 3400 and 3100 cm^{-1}. This suggests that no components were selectively excluded during the electrospinning process. Further observations from the FTIR analysis include a 3328 cm^{-1} band, indicating H–OH stretching of phenols,

a 1628cm^{-1} band indicating the C=O shifting of ketones and aldehydes, a peak at 1378 cm^{-1} equivalent to nitro group twisting with N=O, and bands at 1112 cm^{-1} and 1006 cm^{-1} illustrating esters' C-O stretching. These bands suggest the formation of interactions between phosphate groups and chitosan amine groups, as reported in earlier studies (Bagheri et al., 2022; Ridolfi et al., 2017; Kargarzadeh et al., 2015).

Additionally, aromatic vibrations of compounds found in the green-synthesized silver nanoparticles were detected at 1450 cm^{-1}, 1500 cm^{-1}, and 1600 cm^{-1}, confirming their presence and indicating the binding of silver ions to chitosan functional groups, consistent with findings by Bagheri et al. in 2022. It's noteworthy that the peaks related to Ag NPs were not prominently visible, likely due to their being masked by the broad and strong bond stretches of the chitosan and PEO matrix. Some irregular small peaks suggest the presence of impurities in the samples.

In addition, the substance's amino signals demonstrate its bio-disponibility by demonstrating the constituents' potential to theoretically transmit and exert antibacterial and curative properties through liaisons with hydrogenated -NH groups on microbe cell walls, as discussed in the work of Martínez-Camacho et al. in 2013.

3.4 XRD analysis

The composites of CTS, PEO, and AgNPs displayed distinctive X-ray diffraction patterns (Figure 4). The crystallinity of chitosan (CT), principally due to its primary chain components, was shown by a noticeable peak at 20. In addition, peaks at 77.20, 64.50, 44.30, and 38.00 stand for the (3 1 1), (2 2 0), (2 0 0), and (1 1 1) planes of the face-centred cubic structure of silver nanoparticles (AgNPs), were also noted. These results indicated that the CT + PEO nanofiber matrix included well-dispersed and encapsulated AgNPs (Chen et al., 2019; Ribeiro et al., 2021). These X-ray diffraction results also matched the FTIR study, proving that the composite with 4.0 wt% AgNPs in CT + PEO nanofibers showed a more crystalline phase and a diminished presence of the less crystalline phase. According to Kim's group, the polarization of the nanofibers caused this preference for the phase, which was brought on by the use of a high DC voltage during the electrospinning procedure (Mandal et al., 2011).

3.5 Differential scanning calorimetry analysis

Enthalpy values and peak temperature of the nanofibers are illustrated in Table 1.

Table 1: DSC analysis of the electrospun nanofiber samples.

Nanofiber samples	At melting temperature (T_m)		At glass transition temperature (Tg)	
	T_m (^{0}C)	ΔH (J/g)	T_g (^{0}C)	ΔH (J/g)
CT	179.78	21.45	62.34	185.12
CT + PEO	185.92	18.91	70.45	162.56
CT + PEO + AgNPs	175.64	19.88	64.92	158.43

Figure 3.7 displays DSC thermograms of various electrospun nanofibers. The T_m (melting temperature) and T_g (glass transition temperature) of electrospun nanofibers containing Ag NPs (silver nanoparticles) along with CT (Chitosan) and PEO (Polyethylene Oxide) were slightly lower at 64.92°C and 175.64°C, respectively, compared to the pure CT + PEO nanofibers, which had T_m and T_g values of 70.45°C and 185.92°C. This discrepancy can be due to the polymer chains' conformation and the electrospun nanofibers' high surface-area-to-volume ratio. The T_m of the CT + PEO nanofibrous mat (185.92°C) increased when Ag NPs were added, and the interaction between Chitosan and the PEO matrix was enhanced. In simpler terms, the accumulation of PEO and Ag NPs led to a higher Tm of approximately 185.92°C, and the ΔH value diminished from 21.45 Jg^{-1} to 19.88 Jg^{-1}. Nanofibers are potential options for wound rehabilitation because of their permeable nature and good fluid intake capability. Additionally, their ability to facilitate oxygen exchange plays a crucial role in promoting cell viability, blood vessel renewal, infection control, and proliferation.

Conclusion

This study looked into the blend electrospinning procedure used to produce synthesized AgNP nanofibers from chitosan/PEO/green for use in wound healing applications. The created nanofibers are beadles, porous, and have a nanoscale structure for maximum biocompatibility. The CT + PEO + AgNP combination of electrospun nanofibers displayed excellent-quality fibres with low bead formation due to the substance's elevated surface tension. The nanoparticle loading in nanofibers is confirmed by the FTIR data. The presence of OH absorption bands in the FTIR study results suggests that the electrospinning of the chitosan polysaccharide chains was successful. With an optical fibre diameter of around 150 nm, this consistent and homogeneous architecture is particularly well suited for enveloping silver nanoparticles for prospective uses in the prevention and remediation of microbial-infected wound healing. Overall, the findings of this work indicate that dynamically manufactured microscopic fibres with great biological compatibility, appropriate tensile strength, and a low level of cytotoxicity can be used as a suitable platform for wound-healing applications.

References

Angammana, C.J. and Jayaram, S.H., 2011. Analysis of the effects of solution conductivity on electrospinning process and fiber morphology. *IEEE Transactions on Industry Applications*, *47*(3), pp. 1109-1117.

Anjum, S., Rahman, F., Pandey, P., Arya, D.K., Alam, M., Rajinikanth, P.S. and Ao, Q., 2022. Electrospun biomimetic nanofibrous scaffolds: a promising prospect for bone tissue engineering and regenerative medicine. *International Journal of Molecular Sciences*, *23*(16), p. 9206.

Antunes, B.P., Moreira, A.F., Gaspar, V.M. and Correia, I.J., 2015. Chitosan/arginine–chitosan polymer blends for assembly of nanofibrous membranes for wound regeneration. *Carbohydrate polymers*, *130*, pp. 104-112.

Bagheri, M., Validi, M., Gholipour, A., Makvandi, P. and Sharifi, E., 2022. Chitosan nanofiber biocomposites for potential wound healing applications: Antioxidant activity with synergic antibacterial effect. *Bioengineering & translational medicine*, *7*(1), p.e10254.

Bösiger, P., Richard, I.M., Le Gat, L., Michen, B., Schubert, M., Rossi, R.M. and Fortunato, G., 2018. Application of response surface methodology to tailor the surface chemistry of electrospun chitosan-poly (ethylene oxide) fibers. *Carbohydrate polymers*, *186*, pp. 122-131.

Chen, C., Bai, X., Ding, Y. and Lee, I.S., 2019. Electrical stimulation as a novel tool for regulating cell behavior in tissue engineering. *Biomaterials research*, *23*, pp. 1-12.

Chen, Q.J., Zhou, L.L., Zou, J.Q. and Gao, X., 2019. The preparation and characterization of nanocomposite film reinforced by modified cellulose nanocrystals. *International journal of biological macromolecules*, *132*, pp. 1155-1162.

Cui, C., Sun, S., Wu, S., Chen, S., Ma, J. and Zhou, F., 2021. Electrospun chitosan nanofibers for wound healing application. *Engineered Regeneration*, *2*, pp. 82-90.

Elsoud, M.M.A., Elmansy, E.A. and Abdelhamid, S.A., 2022. Economic and Non-Seasonal Source for Production of Chitin and Chitosan. *J. Chem. Rev*, *4*(3), pp. 222-240.

Ganesh, M., Aziz, A.S., Ubaidulla, U., Hemalatha, P., Saravanakumar, A., Ravikumar, R., Peng, M.M., Choi, E.Y. and Jang, H.T., 2016. Sulfanilamide and silver nanoparticles-loaded polyvinyl alcohol-chitosan composite electrospun nanofibers: Synthesis and evaluation on synergism in wound healing. *Journal of Industrial and Engineering Chemistry*, *39*, pp. 127-135.

Geng, X., Kwon, O.H. and Jang, J., 2005. Electrospinning of chitosan dissolved in concentrated acetic acid solution. *Biomaterials*, *26*(27), pp. 5427-5432.

Jirofti, N., Golandi, M., Movaffagh, J., Ahmadi, F.S. and Kalalinia, F., 2021. Improvement of the wound-healing process by curcumin-loaded chitosan/collagen blend electrospun nanofibers: in vitro and in vivo studies. *ACS Biomaterials Science & Engineering*, *7*(8), pp. 3886-3897.

Kargarzadeh, H., Sheltami, R.M., Ahmad, I., Abdullah, I. and Dufresne, A., 2015. Cellulose nanocrystal: A promising toughening agent for unsaturated polyester nanocomposite. *Polymer*, *56*, pp. 346-357.

Khodadoust, M., Mohebbi-Kalhori, D. and Jirofti, N., 2018. Fabrication and characterization of electrospun bi-hybrid PU/PET scaffolds for small-diameter vascular grafts applications. *Cardiovascular engineering and technology*, *9*, pp. 73-83.

Mandal, D., Yoon, S. and Kim, K.J., 2011. Origin of piezoelectricity in an electrospun poly (vinylidene fluoride-trifluoroethylene) nanofiber web-based nanogenerator and nano-pressure sensor. *Macromolecular rapid communications*, *32*(11), pp. 831-837.

Martínez-Camacho, A.P., Cortez-Rocha, M.O., Graciano-Verdugo, A.Z., Rodríguez-Félix, F., Castillo-Ortega, M.M., Burgos-Hernández, A., Ezquerra-Brauer, J.M. and Plascencia-Jatomea, M., 2013. Extruded films of blended chitosan, low-density polyethylene and ethylene acrylic acid. *Carbohydrate polymers*, *91*(2), pp. 666-674.

Mirhaj, M., Labbaf, S., Tavakoli, M. and Seifalian, A.M., 2022. Emerging treatment strategies in wound care. *International Wound Journal*, *19*(7), pp. 1934-1954.

Pakravan, M., Heuzey, M.C. and Ajji, A., 2012. Core-shell structured PEO-chitosan nanofibers by coaxial electrospinning. *Biomacromolecules*, *13*(2), pp. 412-421.

Pourshahrestani, S., Zeimaran, E., Kadri, N.A., Mutlu, N. and Boccaccini, A.R., 2020. Polymeric hydrogel systems as emerging biomaterial platforms to enable hemostasis and wound healing. *Advanced healthcare materials*, *9*(20), p. 2000905.

Ribeiro, A.S., Costa, S.M., Ferreira, D.P., Calhelha, R.C., Barros, L., Stojković, D., Soković, M., Ferreira, I.C. and Fangueiro, R., 2021. Chitosan/nanocellulose electrospun fibers with enhanced antibacterial and antifungal activity for wound dressing applications. *Reactive and Functional Polymers*, *159*, p. 104808.

Ridolfi, D.M., Lemes, A.P., de Oliveira, S., Justo, G.Z., Palladino, M.V. and Durán, N., 2017. Electrospun poly (ethylene oxide)/chitosan nanofibers with cellulose nanocrystals as support for cell culture of 3T3 fibroblasts. *Cellulose*, *24*, pp. 3353-3365.

Shahid, M.A., Ali, A., Uddin, M.N., Miah, S., Islam, S.M., Mohebbullah, M. and Jamal, M.S.I., 2021. Antibacterial wound dressing electrospun nanofibrous material from polyvinyl alcohol, honey and Curcumin longa extract. *Journal of Industrial Textiles*, *51*(3), pp. 455-469.

Shi, D., Wang, F., Lan, T., Zhang, Y. and Shao, Z., 2016. Convenient fabrication of carboxymethyl

cellulose electrospun nanofibers functionalized with silver nanoparticles. *Cellulose*, *23*, pp. 1899-1909.

Srivastava, C.M., Purwar, R. and Gupta, A.P., 2019. Enhanced potential of biomimetic, silver nanoparticles functionalized Antheraea mylitta (tasar) silk fibroin nanofibrous mats for skin tissue engineering. *International journal of biological macromolecules*, *130*, pp. 437-453.

Stoica, A.E., Chircov, C. and Grumezescu, A.M., 2020. Nanomaterials for wound dressings: an up-to-date overview. *Molecules*, *25*(11), p. 2699.

Tan, L., Zhou, Z., Liu, X., Li, J., Zheng, Y., Cui, Z., Yang, X., Liang, Y., Li, Z., Feng, X. and Zhu, S., 2020. Overcoming multidrug-resistant MRSA using conventional aminoglycoside antibiotics. *Advanced Science*, *7*(9), p. 1902070.

Vandghanooni, S. and Eskandani, M., 2019. Electrically conductive biomaterials based on natural polysaccharides: Challenges and applications in tissue engineering. *International journal of biological macromolecules*, *141*, pp. 636-662.